



## SILVER INFLUENCE OF PHYSICAL AND THERMOLUMINESCENCE PROPERTIES ON LITHIUM-STRONTIUM-BORATE LSBO: AG EXPOSED TO COBALT-60 GAMMA RAY

Hayder. K. Obayes<sup>1,2</sup>, H. Wagiran<sup>1</sup>, R. Hussin<sup>1</sup> and M. A Saeed<sup>1</sup>

<sup>1</sup> Department of Physics Sciences, Faculty of Science, Universiti Teknologi Malaysia, UTM Johor Bahru, Johor, Malaysia

<sup>2</sup> Department of Physics, University of Al-Qadisiya, Iraq

E-Mail: [hayder.physics1@gmail.com](mailto:hayder.physics1@gmail.com)

### ABSTRACT

This work investigates the properties of glow curve of lithium Strontium borate doped silver glass (LSBO: Ag), subjected to Co-60 gamma irradiation. The glass samples were prepared in different compositions based on  $15\%Li_2CO_3 + 2\%SrCO_3 + (83-x)H_3BO_3 + xAgNO_3$ , where  $x = 0.001, 0.003, 0.005, 0.007, 0.009$  and  $0.01$  mol% by traditional melting quenching method at temperature  $1300\text{ }^\circ\text{C}$  for 1 hour. The structural pattern of glass samples has been identified by X-ray diffraction. The XRD pattern shows that the samples are glasses since there is broader peak appearing in the spectral pattern. FESEM images verify the homogeneous and transmitting surface morphology of all samples. Stable glasses with Hurby parameter  $\sim 0.5$  are achieved. EDX spectra determine the accurate elemental compositions in the samples. Physical properties are determined in terms of glass density, molar volume, polaron radius, inter-nuclear distance, and ion concentration. Glass density is found to increase from  $2.45$  to  $2.46\text{ g cm}^{-3}$  after addition of  $AgNO_3$  concentration. The TL intensity at different compositions of lithium borate doped silver glass after exposed to  $50\text{ Gy}$  Co-60 gamma-rays is presented. The results clearly show that the highest TL intensity is found in glass composition of  $0.09$  mol% of  $AgNO_3$ .

**Keywords:** LSBO:Ag, structural-thermale-physics properties, thermoluminescence.

### INTRODUCTION

Silver being a multivalent interacts with oxygen and materializes into different phases such as  $Ag_2O, AgO, Ag_3O_4, Ag_4O_3,$  and  $Ag_2O_3$  (Bielmann *et al.*, 2002). The different crystalline structures of these oxides exhibit many physiochemical, electrochemical, electronic, and optical properties.  $Ag_2O$  and  $AgO$  are the most stable and abundant phases (Garner and Reeves, 1954).  $Ag_2O$  is under extensive investigation because of its many interesting applications. The silver oxide recently got attention due its potential use in optical memories.

Silver oxide has been studied extensively for the applications in electrical, optical and magneto-optical data storage industries. During the past years, the silver oxide electrode applied as a battery material has been developed to achieve better performance in voltage regulation with longer storage life (Passaniti *et al.*, 1995), (Smith *et al.*, 1997). Owing to its larger optical band gap ( $2.5\text{--}3.1\text{ eV}$ ), silver oxide is transparent in the infrared and visible regions to realize a transparent electrode and anti-reflective coating for applications in the opt-electrical field. Furthermore, the silver oxide can be applied in optical and magneto optical data storage. The reflectivity of the silver oxide is higher than  $70\%$  over a very wide wavelength range. This has the advantage for the material to be applied in the short-wavelength optical data storage to replace the commonly used organic storage material.

There are several natural and synthetic borates that are used in many industry applications, due to their high impurity in processing plants and are further treated with more qualified finishing products such as boric acid, anhydrous boric, anhydrous borax, borax pentahydrate, borax decarate, borax decahydrate, and sodium perborate)

in recrystallizer units. However, the variability of borate crystal chemistry (Yu *et al.*, 2002), which allows the researchers to synthesize different types of the borate to use in high technological areas. One of the most important type of borate is the lithium borate that has been synthesized in a powder form, which resulted from the homogenizing a mixture of the stoichiometric quantities of reactants ( $Li_2CO_3$  and  $H_3BO_3$ ) at  $750\text{ }^\circ\text{C}$  for 14 hrs. Lithium borate namely lithium tetraborate and lithium triborate produced by different methods to use for TL dosimetry. Initially lithium borate is a white powder that has an indistinctive order, and it has a melting point of  $917\text{ }^\circ\text{C}$  and solubility is in a moderate range of (1-10%) along with a density of  $2.4\text{ g/cm}^3$ . Lithium borate possesses numerous technological piezoelectricity (Gorelik *et al.*, 2003). Borate glasses are very interesting amorphous materials considering their specific structure and physical properties, lithium borate is rather new in TL dosimetry compared to lithium tetraborate. Thermoluminescent (TL) dosimetry is an important technology utilized to measure the radiation exposure of this synthetic borate. The technological properties of lithium borate are peculiar to crystallization system. In the recent years, thermoluminescent properties of lithium borate  $LiB_3O_5$  have also attracted many attentions from the scientists and researchers for the medical applications, due to their effective atomic number, which is very close to the biological tissue.

The present study is focused on identifying the physical properties of lithium borate glass that is prepared with different concentrations, followed by an irradiation process to come out with analysis the glow curve lithium borate.



## EXPERIMENTAL PROCEDURE

### Sample preparation

The  $\text{Li}_4\text{Sr}(\text{BO}_3)_3$  glasses of compositions  $(85-x)\text{H}_3\text{BO}_3 + 15\%\text{Li}_2\text{CO}_3 + 2\%\text{SrO}_2 + x\text{AgNO}_3$  ( $x = 0.001, 0.003, 0.005, 0.007, 0.009$  and  $0.01$  mol%) were synthesized using melt-quenching technique at different concentrations of strontium ions. The powder of the compounds was weighted and well-mixed using milling machine. The mixture was melted in an alumina crucible for one hr using an electric furnace a NabGmbH at a temperature of  $1300^\circ\text{C}$ . The  $\text{Li}_2\text{CO}_3$  (purity 99.+%),  $\text{H}_3\text{BO}_3$  (purity 99.98%) and  $\text{SrCO}_3$  (purity 99.9%),  $\text{AgNO}_3$  (purity 99%), were supplied by 'Syarikat Pustaka Elit, Johor Bahru, Malaysia'. After completion of melting, the liquid glass was poured and quenched on well-polished pre-heated steel plate. The samples were annealed at  $400^\circ\text{C}$  for three hr to eliminate the mechanical stress. Six samples (A1, A2, A3, A4, A5, and A6) with their compositions are summarized in Table-1.

**Table-1.** Compositions and coded of prepared glass samples.

Samples	Concentration (mol %)			
	$\text{Li}_2\text{CO}_3$	$\text{SrCO}_3$	$\text{H}_3\text{BO}_3$	$\text{AgNO}_2$
1	15	2	82.995	0.001
2	15	2	82.99	0.003
3	15	2	82.97	0.005
4	15	2	82.95	0.007
5	15	2	82.93	0.009
6	15	2	82.91	0.01

### Samples characterizations

The amorphous nature of all samples (at room temperature) was verified using X-ray diffraction (XRD) analysis (Siemens Diffractometer D5000), equipped with diffraction software analysis. It used

$\text{Cu K}\alpha$  radiation ( $\lambda = 1.54 \text{ \AA}$ ) operating at 40 kV and 30 mA. The XRD profiles on powdered samples were collected in the range of  $2\theta = 5-90^\circ$  at a scanning rate of  $0.05^\circ/\text{sec}$ . The particle morphology, purity and the phase homogeneity of these glasses were analyzed via field emission scanning electron microscopy (FESEM). The

information about the chemical purity and elemental traces were detected using EDX measurements.

The irradiation was performed using gamma cell, Gamma Ray GC 220 EX machine. The facility is available at the School of Applied Physics, Faculty of Science and Technology, Universiti Kebangsaan Malaysia. The source of gamma ray irradiation used for the gamma cell was Cobalt-60, which was purchased in 2002 with the original dose rate of  $9.234 \text{ kGy hr}^{-1}$ . However, the current dose rate is  $2.263 \text{ kGy hr}^{-1}$ . For gamma ray irradiation, both the doped and un-doped samples were placed inside the perspex. The samples were put into the irradiating chamber of the Gamma Cell. Before the samples were exposed, the dose and time of irradiation were calculated first

## RESULTS AND DISCUSSIONS

### XRD pattern

Figure-1 displays the XRD patterns of undoped LSBO and doped LSBO: Ag glass samples. The patterns and absence of any sharp peaks verify the amorphous structure (Alajerami *et al.*, 2012; Saidu *et al.*, 2014).

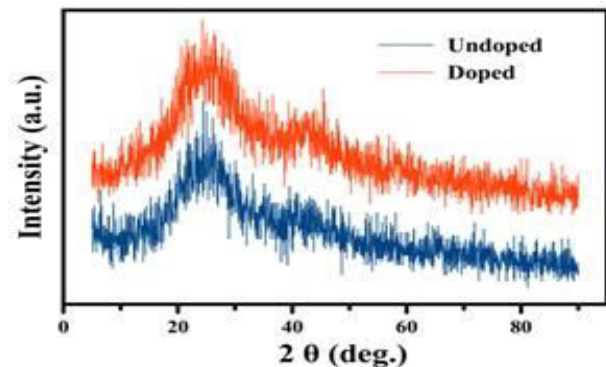


**Figure-1.** XRD Patterns of undoped LSBO and doped LSBO: Ag glass samples.

### FESEM spectra

The FESEM images as illustrated in Figure-2 (2-a) undoped LSBO and, (2-b) doped LSBO: Ag glass samples clearly display the devoid of any grains with homogeneous morphology (Rajesh *et al.*, 2012).

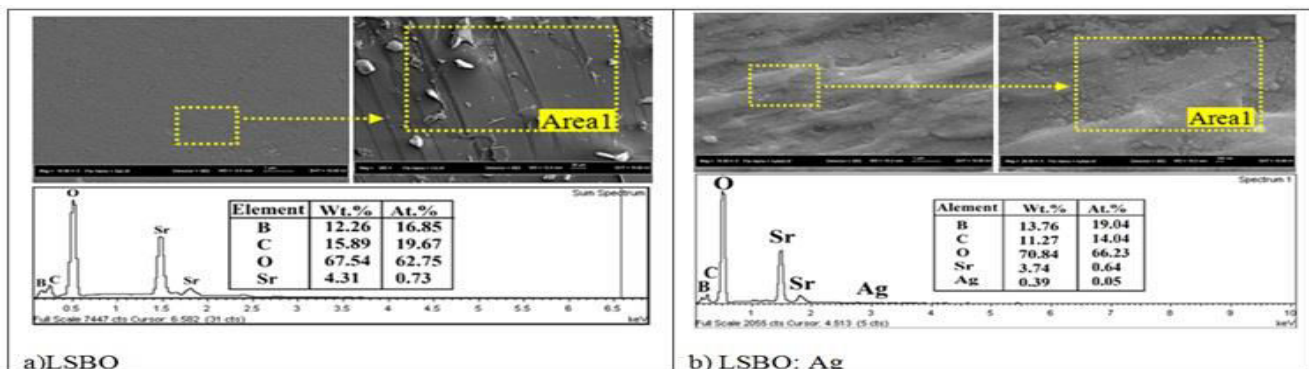


**Figure-2.** FE-SEM images of (a)  $\text{LSBO}_2\text{Sr}$  mol% and, (b)  $\text{LSBO: Ag}$  0.009Ag mol% for glass samples.



### Physics parameters

Concentration-dependent physical properties of undoped LSBO (2Sr mol %) and doped LSBO: Ag (0.009Ag mol %) glass samples are enlisted in Table 2.

Glass density ( $\rho$ ) is determined using Archimedes' principle with toluene as immersion liquid (99.99% purity) from the expression,

$$\rho = \frac{W_a}{W_a - W_i} \times 0.896 \text{ g cm}^{-3} \quad (1)$$

where  $W_a$  and  $W_i$  are the weight of glass in the air and liquid respectively. The density of toluene is found to be  $0.8696 \text{ g cm}^{-3}$  at room temperature ( $27^\circ\text{C}$ ). The density is found to increase from 2.45 to  $2.46 \text{ g cm}^{-3}$  after addition of  $\text{AgO}_2$  concentration. This increase is attributed to the following: (i) conversion of  $[\text{BO}_3]$  triangles into  $[\text{BO}_4]$  tetrahedral, (ii) enhancement of molecular mass of the glass due to insertion of higher atomic weight of silver, and (iii) increase of the oxygen–boron ratio because of the increase in  $\text{AgNO}_3$  concentration.

Molar volume of glasses is calculated from,

$$V_m = \frac{M}{\rho} \text{ cm}^3 \text{ mole}^{-1} \quad (2)$$

where  $V_m$  is the molar volume in  $\text{cm}^3 \text{ mole}^{-1}$  and  $M$  is the molecular weight. Another indication of the glass structure compactness is the increase in density and simultaneous decrease in molar volume ( $32.6078\text{--}31.83 \text{ cm}^3/\text{mol}$ ). This decrease is ascribed to the increase in inter-atomic spacing. This decrease is ascribed to the increase in inter-atomic spacing. This results in accordance to the previous one (Dimitrov and Komatsu, 2010; Tauc, 1974).

Inter-nuclear distance is given by,

$$r_i (\text{\AA}) = \left(\frac{1}{N}\right)^{\frac{1}{3}} \quad (3)$$

The ion concentration is calculated using,

$$N = \frac{\text{mol}\% \times \rho \times NA}{M_i} \left(\frac{\text{Ions}}{\text{cm}^3}\right) \quad (4)$$

where mol% is the mole percent of  $\text{SrCO}_3$  and  $\text{AgNO}_3$ ,  $\rho$  is the glass density,  $NA$  is Avogadro number and  $M_i$  is the average molecular weight of the prepared glass (Ahmed *et al.*, 1984).

According to Shelby (Shelby and Ruller, 1987), three other related physical properties can be calculated after the determination of ion concentration as shown below. The polaron radius (AnChiu *et al.*; Shelby and Ruller, 1987),

$$r_p (\text{\AA}) = \frac{1}{2} \left(\frac{\pi}{6N}\right)^{\frac{1}{3}} \quad (5)$$

**Table-2.** The physical parameters of glass samples.

physical parameters	Glasses samples	
	Undoped LSBO (2Sr mol %)	Doped LSBO: Ag (0.009Ag mol %)
$\rho$	2.45	2.46
$V_m$	31.93	31.83
$N$	$3.77 \times 10^{22}$	$1.70 \times 10^{20}$
$r_i$ ( $\text{\AA}$ )	$2.57 \times 10^{-12}$	$3.82 \times 10^{-11}$
$r_p$ ( $\text{\AA}$ )	$1.86 \times 10^{-12}$	$2.76 \times 10^{-11}$

### TL intensity

The glow curves are particularly important since they are the main indicators of whether a material can be used for the TL dosimetry purpose. It is desired that the glow curve gives a simple, if possible single peak at around  $200^\circ\text{C}$ . The peak observed at low temperature in the proximity of  $100^\circ\text{C}$  fades away quickly and does not yield any information about the radiation content. This maximum is not symmetric, and the half-width of this peak is wide, these properties of shoulder peak imply that it has a complicated nature. Such maximum is claimed to root from the superposition of a number of local trapping at a certain level (Pekpak *et al.*, 2010). In a similar way peaks observed around  $300^\circ\text{C}$  are not assigned to good TL properties. Another custom to be followed is performing the readings after 24 hours from the irradiation process (Pekpak, *et al.*, 2010). Figure-3 shows a significant property considering the radiation dosimetry potential that LSBO: Ag has the highest thermoluminescence peak of  $94.10 \text{ nC g}^{-1}$ . Based on these results, the best compositions for these glasses LSBO:Ag are those with  $[15\% \text{Li}_2\text{CO}_3 + 82.991\% \text{H}_3\text{BO}_3 + 2\% \text{SrO}_2 + 0.009\% \text{AgNO}_3]$ . The optimization of heating rate was recorded with different heating rate. Figure-4 shows the highest TL intensity at heating rate 3 with lower standard deviation.

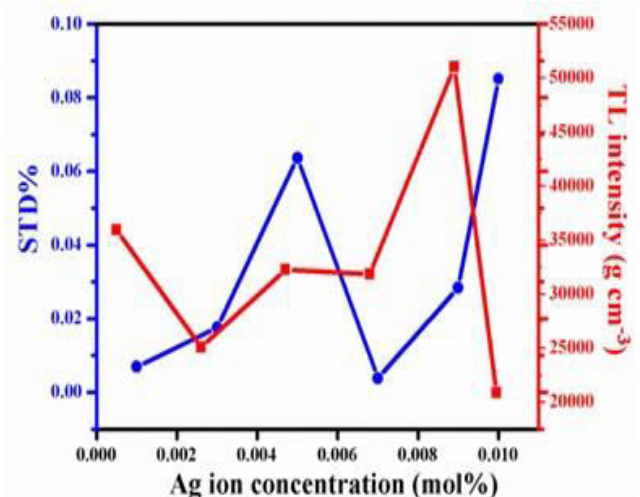


**Figure-3.** TLD responses of LSBO: Ag with versus concentration of  $\text{AgNO}_3$ .





www.arpnjournals.com

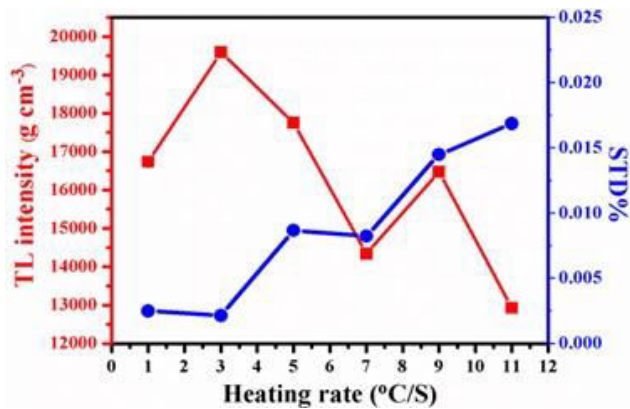


**Figure-4.** Optimization heating rate of LSBO: Ag glass samples.

## CONCLUSIONS

Silver ions concentration dependent structural and thermal properties of LSBO: Ag glasses are successfully demonstrated. The highest TL response was found at concentration of (0.009 mol% Ag). Thermally stable and synthesized LSBO: Ag glasses are reported via conventional melt quenching method. Structures are determined via XRD and FESEM measurements. Elemental compositions are detected via EDX. Physical, structural are strongly influenced by the incorporation of Silver ions in the glass network. The values for density, molar volume, ion concentration, inter nuclear distance, polaron radius and thermal parameters of these glasses are also compared. The thermal stability is found to decrease with addition of Ag. The admirable features of the results suggest that the present glass composition has potential for the fabrication of solid state lasers, photonic devices, and optical fibers

## ACKNOWLEDGEMENTS

The author(s) would like to thank the Malaysian Ministry of Education (MOE) and Universiti Teknologi Malaysia for providing the financial support and facilities for this research, under Grant No. R.J130000.7826.4F490. Further one of the author (Hayder Khudhair Obayes.) would like to thank UTM for the financial support by IDF reference UTM.J.10.01/13.14/1/128.

## REFERENCES

- [1] Ahmed, M., Hogarth, C. and Khan, M. (1984). A study of the electrical and optical properties of the GeO<sub>2</sub>-TeO<sub>2</sub> glass system. *Journal of materials science*. 19(12), 4040-4044.
- [2] Alajerami, Y. S. M., Hashim, S., Wan Hassan, W. M. S. and Ramli, A. T. (2012). The effect of titanium oxide on the optical properties of lithium potassium borate glass. *Journal of Molecular Structure*. 1026, 159-167.
- [3] AnChiu, C., Xian, W. and Moss, C. F. (2008). Flying in silence: Echolocating bats cease vocalizing to avoid

sonar jamming. *Proceedings of the National Academy of Sciences of the United States of America*. 105(35), 13116-13121.

- [4] Bielmann, M., Schwaller, P., Ruffieux, P., Gröning, O., Schlapbach, L. and Gröning, P. (2002). AgO investigated by photoelectron spectroscopy: Evidence for mixed valence. *Physical Review B*. 65(23), 235431.
- [5] Dimitrov, V. and Komatsu, T. (2010). An interpretation of optical properties of oxides and oxide glasses in terms of the electronic ion polarizability and average single bond strength. *J. Univ. Chem. Technol. Metall.* 45(3), 219-250.
- [6] Garner, W. and Reeves, L. (1954). The thermal decomposition of silver oxide. *Trans. Faraday Soc.* 50, 254-260.
- [7] Gorelik, V., Vdovin, A. and Moiseenko, V. (2003). Raman and hyper-Rayleigh scattering in lithium tetraborate crystals. *Journal of Russian Laser Research*. 24(6), 553-605.
- [8] Passaniti, J., Megahed, S. and Linden, D. (1995). *Handbook of batteries*. McGraw-Hill, New York.
- [9] Pekpak, E., Yilmaz, A. and Özbayoglu, G. (2010). An overview on preparation and TL characterization of lithium borates for dosimetric use. *Open Mineral Processing Journal*. 3(1), 14-24.
- [10] Rajesh, D., Balakrishna, A., Seshadri, M. and Ratnakaram, Y. (2012). Spectroscopic investigations on Pr<sup>3+</sup> and Nd<sup>3+</sup> doped strontium-lithium-bismuth borate glasses. *Spectrochimica Acta Part A: Molecular and Biomolecular Spectroscopy*. 97, 963-974.
- [11] Saidu, A., Wagiran, H., Saeed, M. and Alajerami, Y. (2014). Structural properties of Zinc Lithium borate glass. *Optics and Spectroscopy*. 117(3), 396-400.
- [12] Shelby, J. E. and Ruller, J. (1987). Properties and structure of lithium germanate glasses. *Physics and chemistry of glasses*. 28(6), 262-268.
- [13] Smith, D. F., Graybill, G. R., Grubbs, R. K. and Gucinski, J. A. (1997). New developments in very high rate silver oxide electrodes. *Journal of power sources*. 65(1), 47-52.
- [14] Tauc, J. (1974). *Amorphous and liquid semiconductors*. Plenum, London, NY.
- [15] Yu, Z.-T., Shi, Z., Chen, W., Jiang, Y.-S., Yuan, H.-M. and Chen, J.-S. (2002). Synthesis and X-ray crystal structures of two new alkaline-earth metal borates: SrBO<sub>2</sub>(OH) and Ba<sub>3</sub>B<sub>6</sub>O<sub>9</sub>(OH)<sub>6</sub>. *Journal of the Chemical Society, Dalton Transactions*. (9), 2031-2035.